Applied Catalysis B: Environmental 89 (2009) 551–556

Contents lists available at ScienceDirect

Applied Catalysis B: Environmental

journal homepage: www.elsevier.com/locate/apcatb

Visible light-induced photocatalytic activity of delafossite $AgMO_2$ (M = Al, Ga, In) prepared via a hydrothermal method

Hui Dong, Zhaohui Li *, Ximing Xu, Zhengxin Ding, Ling Wu, Xuxu Wang, Xianzhi Fu *

Research Institute of Photocatalysis, Fuzhou University, State Key Laboratory Breeding Base of Photocatalysis, #523 Gongye Road, Fuzhou 350002, PR China

ARTICLE INFO

Article history:
Received 26 October 2008
Received in revised form 28 December 2008
Accepted 22 January 2009
Available online 3 February 2009

Keywords:
Hydrothermal
Delafossite
$AgMO_2$
Visible light
Photocatalytic

ABSTRACT

Delafossite-structured oxides $AgMO_2$ (M = Al, Ga, In) were successfully synthesized using fluoro(ethylene-propylene) (FEP) pouch via a facile hydrothermal method. The obtained samples were characterized by X-ray diffraction (XRD), BET surface area measurement, UV–vis diffuse reflectance spectroscopy (DRS), scanning electron microscopy (SEM) and X-ray photoelectron spectroscopy (XPS). The photocatalytic activity of the as-prepared samples was evaluated by the degradation of rhodamine B (RhB) and methyl orange (MO) under visible light irradiation. All three samples showed photocatalytic activity for RhB and MO degradation under visible light irradiations and their photocatalytic activity followed the order of $AgInO_2 > AgGaO_2 > AgAlO_2$. The relative high photocatalytic activity of $AgInO_2$ can be attributed to its high quantity of the surface hydroxyl groups. The photocatalytic mechanism of $AgInO_2$ was proposed and its stability was also investigated.

1. Introduction

Semiconductor photocatalysts have been widely employed in the treatment of all kinds of organic contaminants. Photocatalysis has many advantages over other treatment methods. It is environmentally friendly, capable of performing at room temperature and it can treat organic pollutants at extremely low concentrations. However, with a relatively wide band gap (3.2 eV), the commonly used photocatalyst TiO_2 can only absorb a small fraction of solar energy and thus restrict its practical applications [1–8]. To develop a photocatalyst with high activity under visible light is indispensable in view of the efficient utilization of solar energy.

Over the past several years, considerable effort has been made to increase the visible light-driven photocatalytic activity of the photocatalysts [9–11]. Two strategies have been employed in the design of visible light-driven photocatalysts. One strategy involves the chemical modifications on a UV-active photocatalyst, including doping of foreign elements or coupling with a narrow band gap semiconductor. The other is to develop new single-phase oxide photocatalysts with visible light-driven photocatalytic activity. Bi_2WO_6 [12], $BiVO_4$ [13], MIn_2O_4 (M = Ca, Sr and Ba) [14], $CaBi_2O_4$ [15] and β-$AgAlO_2$ [16], etc. have been prepared and their visible light-induced photocatalytic activities in the degradation of organic pollutants have been explored.

Recently, $AgGaO_2$ with a delafossite structure has been reported to show photocatalytic activity toward the degradation of 2-propanol under both visible light and UV light irradiation [17]. Delafossite-structured oxides, denoted by AMO_2, in which A refers to d^{10} metal ions (Cu^+ or Ag^+), are successful materials for p-type transparent conductors (TCO) [18,19]. Delafossite-structured oxides usually have a layered structure and can be further classified into rhombohedral 3R- ($R\bar{3}m$) or hexagonal 2H- ($P6_3/mmc$) polytype based on the stacking of the alternating layers (Fig. 1) [20,21]. In the delafossite structure, the O–A–O dumbbell layers are interweaved with edge-sharing MO_6 blocks along the *c*-axis. These O–A–O dumbbell layers and MO_6 layers can act as separate conduction paths for holes and electrons respectively. Besides this, the oxygen atom builds an OM_3A tetrahedron, forming an O-$2sp^3$ orbital [18,19,22]. Calculations also reveal that delafossite oxides possess a highly dispersed valence band and thus a higher hole mobility [17]. All these structural features, which are related to the effective charge carrier separations and mobility, are advantageous to the photocatalytic activity. However, until now, among the delafossites oxides, only $AgGaO_2$ has been reported to show photocatalytic activity in the degradation of organic pollutants [17]. Theoretical calculations have revealed that in the AMO_2 delafossite oxides, the M-site ions can influence the band gap and the electronic structure, which is expected to result in the difference of the photocatalytic activity [23]. Therefore it is interesting to explore the photocatalytic activity of other

* Corresponding authors. Tel.: +86 591 83738608; fax: +86 591 83738608.
E-mail addresses: zhaohuili1969@yahoo.com (Z. Li), xzfu@fzu.edu.cn (X. Fu).

0926-3373/$ – see front matter © 2009 Elsevier B.V. All rights reserved.
doi:10.1016/j.apcatb.2009.01.018

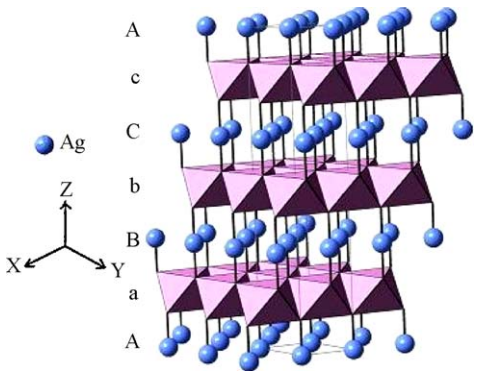

Fig. 1. Schematic representation of the delafossite structure (ABO_2) for the "3R" polytype ($R\bar{3}m$) with AaBbCcAa ... stacking along the *c*-axis. The "2H" polytype ($P6_3/mmc$) has an alternate AaBbAa ... stacking sequence. The polyhedra and spheres represent $B^{3+}O_6$ distorted octahedra and linearly coordinated A^+ cations, respectively.

delafossite-structured metal oxides for the degradation of organic pollutants.

Due to the decomposition of Ag_2O at temperature higher than 300 °C, it is difficult to obtain silver delafossites by conventional solid-state reaction. Alternative synthetic methods, like metathetical (cation-exchange) [24], oxidizing flux [25] and high temperature hydrothermal reactions [26] have been reported in preparing silver delafossites. However, limitations for these synthetic methods exist. For example, the metathesis reaction often leads to the formation of highly stable metal halides (e.g., AgCl) with little or no delafossite-type oxide. Oxidizing flux reaction can give the delafossite phase with high yield, but it often results in the presence of a second phase like Ag_2O. Hydrothermal reactions carried out at high temperature (500–700 °C) and high pressure (3000 atm) only produce small amounts of the target delafossite mixed with Ag_2O. Besides this, similar to most hydrothermal technique performed under both high pressure and high temperature, the use of sealed, thin walled gold or platinum tubes limits the mass production of the products. It is until recently that the low temperature hydrothermal technique using the fluoro(ethylene-propylene) (FEP) Teflon pouch were reported to synthesize numerous silver delafossites oxides [27,28]. This kind of closed system synthesis offers a facile low temperature approach to the production of pure silver delafossite oxides and can be expanded to the syntheses of other metal oxides.

In this study, we reported the photocatalytic activity of delafossite-structured oxides $AgMO_2$ (M = Al, Ga, In) prepared using FEP pouch via a hydrothermal reaction. The as-prepared samples were fully characterized and their photocatalytic performance under visible light irradiations was investigated. The effect of M^{3+} on the photocatalytic property of $AgMO_2$ (M = Al, Ga, In) was also studied. Delafossite-structured oxide $AgInO_2$, even with a low specific surface area, exhibits high and stable photocatalytic activity under visible light irradiations.

2. Experimental

2.1. Syntheses

All of the reagents were analytical grade and used without further purifications. Polycrystalline silver delafossite oxides were prepared following a reported method [27–29]. For preparing $AgAlO_2$, Ag_2O (0.301 g, 1.3 mmol) and Al_2O_3 (0.133 g, 1.3 mmol) were placed along with fused NaOH into a fluoro(ethylene-propylene) Teflon pouch. The pouch was sealed and placed in a 100 ml Teflon-lined autoclave filled with 50 ml of deionized water. The pressure vessel was sealed and heated at 150 °C for 5 h to allow water to enter the permeable membrane of the pouch and dissolve NaOH, followed by increasing to 210 °C. The reaction temperature was held constant for 60 h with subsequent cooling to room temperature. The pouch was opened and polycrystalline $AgAlO_2$ were recovered by filtration, followed by a rinse using deionized water to remove any unreacted NaOH. The solid collected was dried at 80 °C for at least 12 h. A similar procedure can be applied to the preparations of $AgGaO_2$ and $AgInO_2$, except that the reaction temperature for $AgGaO_2$ is 180 °C and that for $AgInO_2$ is 200 °C.

2.2. Characterizations

X-ray diffraction (XRD) patterns were collected on a Bruker D8 Advance X-ray diffractometer with Cu Kα radiation. The accelerating voltage and the applied current were 40 kV and 40 mA, respectively. Data were recorded at a scan rate of $0.02^\circ\ 2\theta\ s^{-1}$ in the 2θ range from 10° to 70°. The Brunauer–Emmett–Teller (BET) surface areas were determined by nitrogen adsorption–desorption isotherm measurements at 77 K on a Quantachrome NOVA200E system. UV–vis diffuse reflectance spectra (DRS) were recorded on a Varian Cary 500 Scan UV–vis–NIR spectrometer with $BaSO_4$ as the background between 200 and 800 nm. Morphology of the samples was characterized by field emission scanning electron microscopy (SEM) (JSM-6700F). X-ray photoelectron spectroscopy (XPS) measurements were performed on a PHI Quantum 2000 XPS system with a monochromatic Al Kα source and a charge neutralizer. All the binding energies were referred to the C 1s peak at 284.8 eV of the surface adventitious carbon. The fluorescence spectra were measured on an FL/FS 900 time-resolved fluorescence spectrometer.

2.3. Photocatalytic activity measurements

The photocatalytic activity of silver delafossites $AgMO_2$ (M = Al, Ga, In) was evaluated by the decomposition of RhB and MO in an aqueous solution visible light irradiation. For RhB, 80 mg of photocatalyst was added into 80 ml of RhB solution (10^{-5} mol/l). 500 W tungsten halogen lamp was positioned inside a cylindrical Pyrex vessel and surrounded by a circulating water jacket (Pyrex) to cool the lamp. A cutoff filter was placed outside the Pyrex jacket to completely remove all wavelengths less than 420 nm to ensure the irradiation with visible light only. Prior to irradiation, the suspensions were magnetically stirred in the dark for ca. 4 h to ensure the establishment of an adsorption/desorption equilibrium. At given irradiation time intervals, 4 ml of the suspensions were collected, centrifuged, and filtered through a Millipore filter to separate the photocatalyst particles. The degraded solutions of RhB were analyzed by a Varian Cary 500 Scan UV–vis spectrophotometer and the absorption peaks at 554 nm for RhB were monitored. The percentage of degradation is reported as C/C_0. C is the absorption of RhB at each irradiated time interval of the maximum peak of the absorption spectrum at wavelength 554 nm. C_0 is the absorption of the starting concentration when adsorption/desorption equilibrium was achieved. The measurement of the photocatalytic activity of $AgMO_2$ for the degradation of MO is similar to that of RhB except that the initial concentration of MO is 20 ppm. The absorption peak at 464 nm for MO was monitored.

3. Results and discussion

3.1. Characterizations

Fig. 2 shows the XRD patterns of $AgMO_2$ (M = Al, Ga and In) prepared through the hydrothermal process. The XRD patterns of the as-prepared products can be indexed as pure-phase 3R ($R3m$)

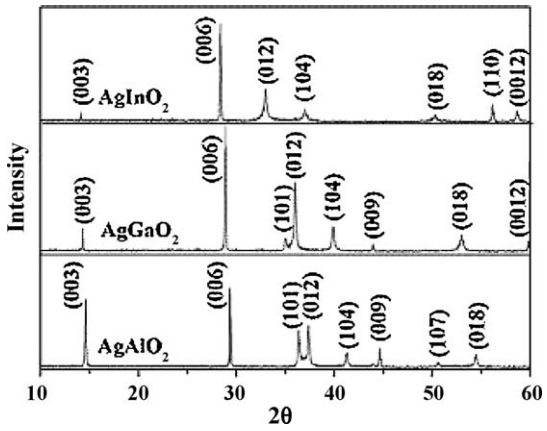

Fig. 2. XRD patterns of $AgMO_2$ (M = Al, Ga, In): (a) $AgAlO_2$, (b) $AgGaO_2$, and (c) $AgInO_2$.

silver delafossite [30]. The diffraction peaks are intense and sharp, indicating that the obtained $AgMO_2$ are well crystallized. All three samples exhibit almost the same XRD patterns except that the diffraction peaks for $AgGaO_2$ and $AgInO_2$ are shifted to low angles compared to those of $AgAlO_2$. This indicates an increase in the lattice parameters with the increase of the ionic radii of M^{3+} (from Al to Ga to In). The BET surface areas are 0.85, 1.38 and 0.62 m^2/g for $AgAlO_2$, $AgGaO_2$ and $AgInO_2$, respectively.

The SEM images of the as-prepared samples are shown in Fig. 3. The obtained $AgAlO_2$ consists mostly of hexagonal plates with edge length of about 3–8 μm and thickness of 200–500 nm (Fig. 3a), with some small pieces attached to these plates. The $AgGaO_2$ sample consists of many dodecahedrons in the size of 200–800 nm (Fig. 3b). The as-obtained $AgInO_2$ sample also consists of hexagonal plates with a typical thickness of about 0.4–1.5 μm and edge length in the range of 1–5 μm (Fig. 3c).

The typical UV–vis diffuse reflection spectra of the hydrothermally synthesized $AgAlO_2$, $AgGaO_2$ and $AgInO_2$ were measured by UV–vis spectrometry (Fig. 4). Since all three oxides belong to the indirect semiconductors [17,31], the relationship between the absorption coefficient and the band gap energy can be described by the formula: $(F(R)h\nu)^{1/2} = A(h\nu - E_g)$, where $h\nu$ and E_g are photon energy and optical band gap energy respectively, and A is the characteristic constant of the semiconductors [32]. From the equation, $(F(R)h\nu)^{1/2}$ has a linear relationship with $h\nu$. By extrapolation of the linear relation to $(F(R)h\nu)^{1/2} = 0$, E_g of the semiconductor can be obtained. Based on the above formula, the band gap was estimated to be 3.2, 2.4 and 2.0 eV for $AgAlO_2$, $AgGaO_2$ and $AgInO_2$ respectively, showing a decrease in the band gap with the increase of the M^{3+} radius (M = Al, Ga and In) (Fig. 4b). The band gap trend in $AgMO_2$ (M = Al, Ga and In) is similar to that reported in $CuMO_2$ (M = Al, Ga and In) as calculated by the ab initio calculations [23]. The estimated band gaps of $AgAlO_2$, $AgGaO_2$ and $AgInO_2$ are consistent with their color (white for $AgAlO_2$, olive green for $AgGaO_2$ and bright orange for $AgInO_2$).

3.2. Photocatalytic activity

The photocatalytic activity of the as-prepared $AgMO_2$ was evaluated by the degradation of RhB under visible light irradiations. Temporal changes in the concentration of RhB as monitored by the maximal absorption in UV–vis spectra at 554 nm over $AgMO_2$ were shown in Fig. 5a. After visible light irradiations for 360 min, almost no RhB was degraded without $AgMO_2$ and only 19% of RhB was degraded at the presence of $AgAlO_2$. In the case of $AgGaO_2$, about 78% of RhB were degraded after being irradiated for 360 min, while for $AgInO_2$, 100% of RhB were decomposed after only 240 min visible light irradiations. This indicates that all $AgMO_2$ exhibit photocatalytic activity for the degradation of RhB under visible light irradiations and the photocatalytic activity follows the order of $AgInO_2 > AgGaO_2 > AgAlO_2$. The temporal

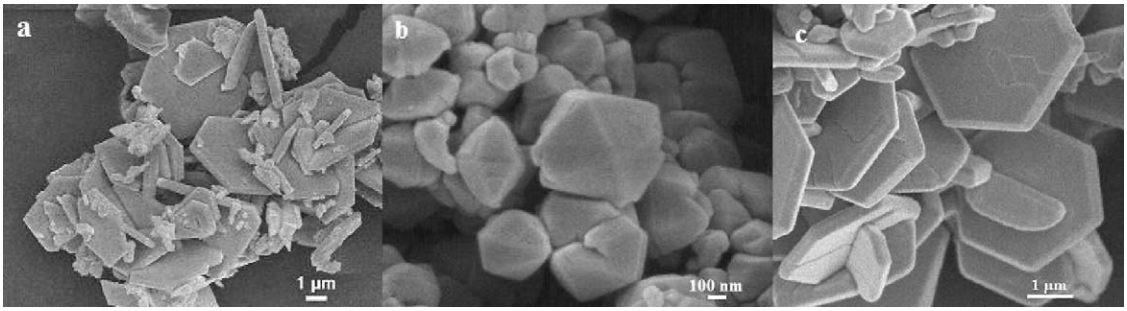

Fig. 3. SEM images of (a) $AgAlO_2$, (b) $AgGaO_2$, and (c) $AgInO_2$.

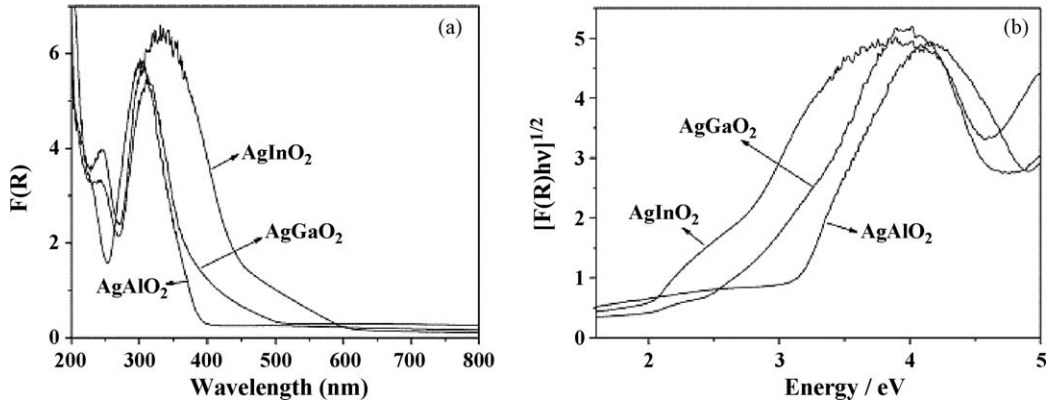

Fig. 4. (a) UV–vis diffuse reflectance spectra of $AgMO_2$ (M = Al, Ga, In) and (b) estimation of band gap energy (E_g) of $AgMO_2$ (M = Al, Ga, In).

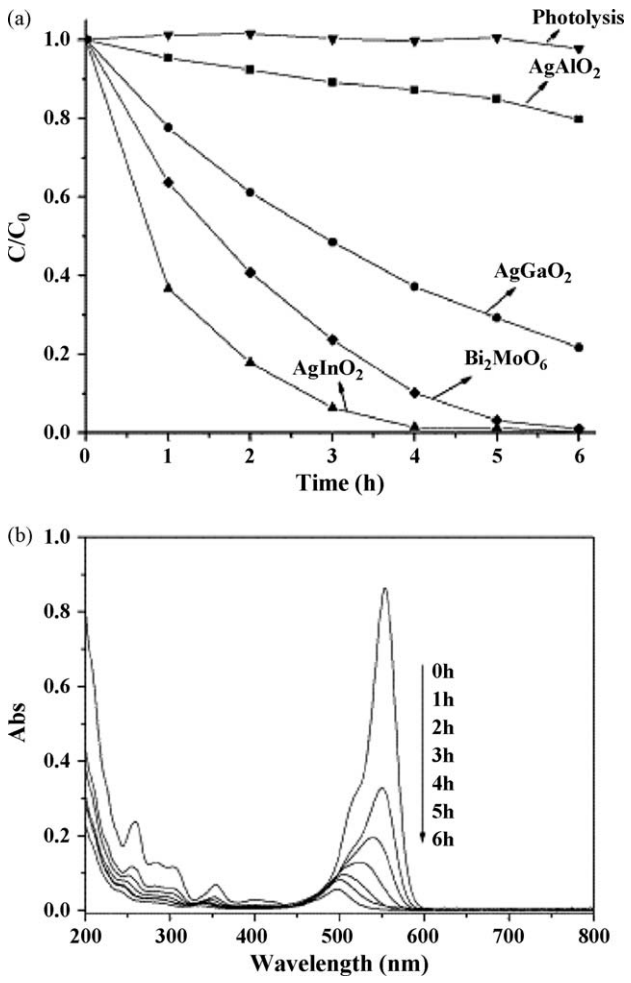

Fig. 5. (a) Temporal changes of RhB concentration as monitored by the UV–vis absorption spectra at 554 nm on $AgMO_2$ (M = Al, Ga, In) and Bi_2MoO_6 and (b) temporal absorption spectral patterns of RhB during the photodegradation process on $AgInO_2$.

evolution of the spectral changes taking place during the photodegradation of RhB over $AgInO_2$ was shown in Fig. 5b. It is found that the main absorbance of RhB (at 554 nm) gradually shifted to shorter wavelength during the irradiations and finally reached 496 nm. This hypsochromic shift in λ_{max} of RhB corresponds to a step-by-step de-ethylation of RhB and the peak centered at 496 nm is assigned to the absorbance of rhodamine, the completely de-ethylated product of RhB [33]. Upon further irradiations the intensity of the peak at 496 nm decreased and indicated that the de-ethylated product of RhB can further be photodegraded to small molecules. In the meantime, the color of the suspension changed gradually from pink to colorless. The photocatalytic activity of $AgInO_2$ is higher than that of microwave-solvothermally prepared Bi_2MoO_6, another visible light photocatalyst we reported previously [34]. The photocatalytic activity of $AgMO_2$ (M = Al, Ga and In) toward another typical dye MO follows a similar order of $AgInO_2 > AgGaO_2 > AgAlO_2$ (Supporting Materials Fig. S1).

The trend of the photocataytic activity among the $AgMO_2$ (M = Al, Ga and In) cannot be simply explained by their band gap. It is not difficult to understand why $AgAlO_2$ showed the lowest photocatalytic activity under visible light irradiations. With a band gap of 3.2 eV, $AgAlO_2$ cannot be excited by the visible light and the degradation of RhB over $AgAlO_2$ under visible light irradiation is caused by the photosensitization with dye as a sensitizer. However, both $AgGaO_2$ and $AgInO_2$ can be excited by the visible light, and with a higher band gap compared with $AgInO_2$ (2.4 eV for $AgGaO_2$ and 2.0 eV for $AgInO_2$), $AgGaO_2$ is expected to show higher photocatalytic activity. This is not consistent with the experimental result. This implies that factors other than band gap may account for the difference in the photocatalytic activity between $AgInO_2$ and $AgGaO_2$.

To explore this, X-ray photoelectron spectroscopy was carried out on the as-prepared $AgGaO_2$ and $AgInO_2$ to determine the oxidation state of the present elements and the results were shown in Fig. 6. Characteristic binding energy (BE) values of 368.1 eV for Ag $3d_{5/2}$ and 374.1 eV for Ag $3d_{3/2}$ are observed for both $AgGaO_2$ and $AgInO_2$ and indicates that in both samples Ag exist as Ag^+ (Fig. 6a) [35,36]. The characteristic binding energy value of 19.2 eV for Ga 3d indicates a trivalent oxidation state for Ga (Fig. 6b) [37]. The In $3d_{5/2}$ and In$3d_{3/2}$ peaks are observed at 444.3 and 451.9 eV, respectively, matching well with that of In^{3+} (Fig. 6c) [38]. This indicates that the as-prepared samples are pure phase $AgGaO_2$ and $AgInO_2$. However, the high-resolution XPS spectra of the as-prepared $AgGaO_2$ and $AgInO_2$ in the O 1s region are different. It is generally accepted that the O 1s peaks can be deconvoluted into oxygen lattice (O^{2-}) at a lower binding energy and surface adsorbed oxygen (O^-) at a higher bonding energy. The adsorbed oxygen (O^-) is believed to exist as surface hydroxyl groups and its quantity is proportional to the quantity of generated $^{\bullet}OH$ radicals [39,40]. By deconvoluting the O 1s peaks in the high-resolution XPS spectra of $AgGaO_2$ and $AgInO_2$ to the peak at 529.8 and 531.6 eV, we found that the ratio of the peak assigned to the surface adsorbed oxygen (531.6 eV) is larger in $AgInO_2$ than that in $AgGaO_2$ (Fig. 6d). This implies that compared to $AgGaO_2$, $AgInO_2$ possess more surface hydroxyl groups. When illuminated, the surface hydroxyl groups are expected to react with the valence holes and therefore more surface hydroxyl groups are expected to lead to more $^{\bullet}OH$ radicals. In this way, more $^{\bullet}OH$ radicals can be generated on $AgInO_2$ than on $AgGaO_2$. Therefore $AgInO_2$ can exhibit higher photocatalytic activity than $AgGaO_2$. This result also implies that the $^{\bullet}OH$ radicals may be the main oxidative species in the photocatalytic degradation of RhB over the $AgMO_2$.

However, the generation of the $^{\bullet}OH$ radicals requires that the photogenerated holes should have strong enough oxidizing ability to react with the surface hydroxyl group. To corroborate the assumption that $^{\bullet}OH$ radicals are really generated over the visible light illuminated $AgInO_2$, terephthalic acid (TA) photoluminescence probing technique was used to detect the generated $^{\bullet}OH$ radicals. TA reacts with $^{\bullet}OH$ radicals to give a highly luminescent TAOH and could be used as a sensitive probe in detecting $^{\bullet}OH$ radicals [41].

The change of the fluorescent signal corresponding to TAOH over the illuminated $AgInO_2$ in terephthalic acid solution was shown in Fig. 7. It is observed that the intensity of the fluorescence at 426 nm increased gradually and indicated the formation of $^{\bullet}OH$ radicals in the visible light illuminated $AgInO_2$. On the contrary, no fluorescent signal was observed in absence of the photocatalyst under otherwise similar condition. The terephthalic acid probe method confirms that photogenerated holes in $AgInO_2$ do oxidize hydroxyl groups to give $^{\bullet}OH$ radicals under visible light illuminations and suggests that the RhB degradation proceed mainly via the $^{\bullet}OH$ radical way.

3.3. Stability

$AgInO_2$ exhibits the highest photocatalytic activity among the $AgMO_2$ delafossite series and can be a candidate for visible light-induced photocatalysis. Its stability during the photocatalytic reactions is important in view of its application. Therefore the stability of $AgInO_2$ was investigated and the result was shown in

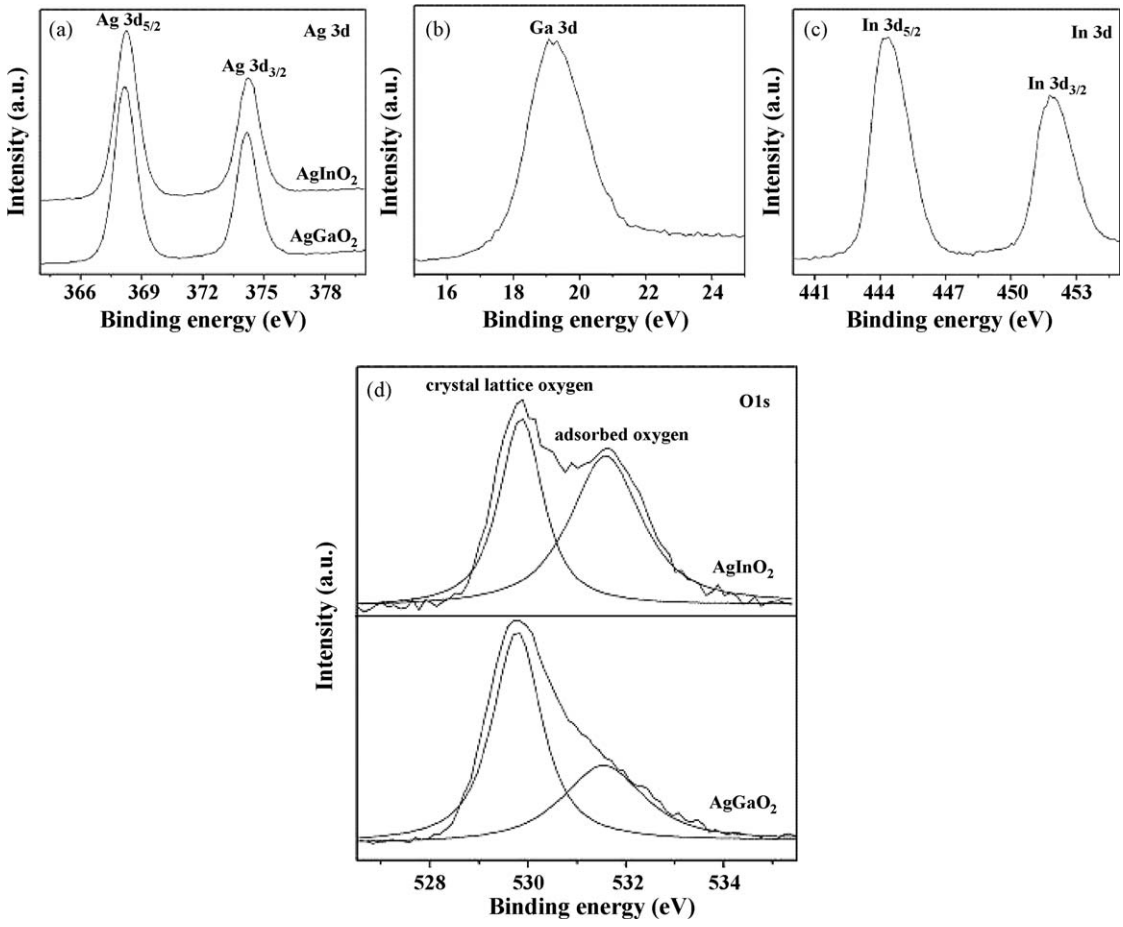

Fig. 6. High-resolution XPS spectra of (a) Ag 3d of $AgGaO_2$ and $AgInO_2$, (b) Ga 3d of $AgGaO_2$, (c) In 3d of $AgInO_2$, and (d) O 1s of $AgGaO_2$ and $AgInO_2$.

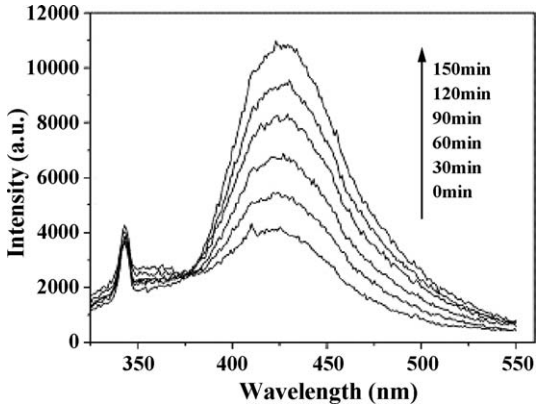

Fig. 7. •OH-trapping PL spectra of $AgInO_2$/TA solution.

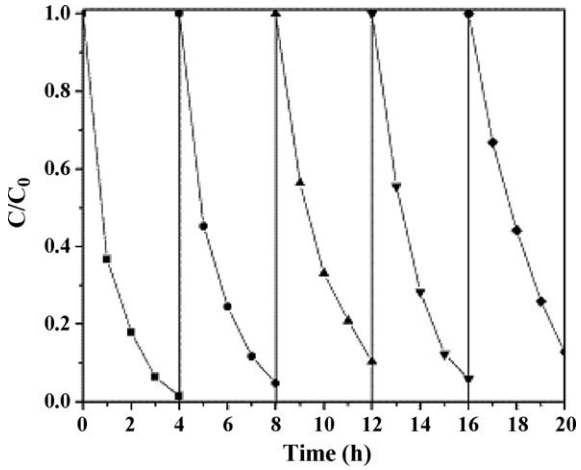

Fig. 8. Cycling runs in the photocatalytic degradation of RhB in the presence of $AgInO_2$ under visible light irradiations.

Fig. 8. Although the photocatalytic activity of $AgInO_2$ was a little lower after the first run, there was no obvious loss of photocatalytic activity for the next four runs. In addition to this, the XRD and XPS of $AgInO_2$ after reacted for times times are almost similar to those of the fresh one (Supporting Materials Figs. S2 and S3). This indicates that $AgInO_2$ is stable during the photocatalytic reaction.

4. Conclusions

Delafossite-structured oxides $AgMO_2$ (M = Al, Ga, In) have been successfully synthesized by a facile hydrothermal technique. All three samples show photocatalytic activity for RhB and MO degradation under visible light and their photocatalytic activity follows the order of $AgInO_2 > AgGaO_2 > AgAlO_2$. The relative high photocatalytic activity of $AgInO_2$ can be attributed to its high quantity of the surface hydroxyl groups. $AgInO_2$ show high stability during the photocatalytic reaction. The photocatalytic degradation of RhB and MO over $AgInO_2$ proceed mainly via the •OH radical way.

Acknowledgments

The work was supported by National Natural Science Foundation of China (20537010 and 20677009), National Basic Research

Program of China (973 Program: 2007CB613306, 2007CB616907), grant from Fujian Province (E0710009). Z. Li thanks program for New Century Excellent Talents in University (NCET-05-0572), State Education Ministry of PR China.

Appendix A. Supplementary data

Supplementary data associated with this article can be found, in the online version, at doi:10.1016/j.apcatb.2009.01.018.

References

[1] A. Mills, R.H. Davies, D. Worsley, Chem. Soc. Rev. 22 (1993) 417.
[2] M.R. Hoffman, S.T. Martin, W. Choi, D.W. Bahnemann, Chem. Rev. 95 (1995) 69.
[3] A. Fujishima, T.N. Rao, D.A. Tryk, J. Photochem. Photobiol. C 1 (2000) 1.
[4] A.L. Linsebigler, G. Lu, J.T. Yates Jr., Chem. Rev. 95 (1995) 735.
[5] A. Fujishima, K. Hashimoto, T. Watanabe, Photocatalysis Fundamentals and Applications, 1st ed., BKC, Tokyo, 1999.
[6] M. Kaneko, I. Okura, Photocatalysis, Science and Technology, Springer, Berlin, 2002.
[7] N. Serpone, E. Pelizzetti, Photocatalysis: Fundamentals and Applications, Wiley, New York, 1989.
[8] M.A. Fox, M.T. Dulay, Chem. Rev. 93 (1993) 341.
[9] R. Asahi, T. Morikawa, T. Ohwaki, K. Aoki, Y. Taga, Science 293 (2001) 269.
[10] W. Zhao, W. Ma, C. Chen, J. Zhao, Z. Shuai, J. Am. Chem. Soc. 126 (2004) 4782.
[11] H. Kisch, W. Macyk, ChemPhysChem 3 (2002) 399.
[12] H. Fu, C. Pan, W. Yao, Y. Zhu, J. Phys. Chem. B 109 (2005) 22432.
[13] L. Zhang, D.R. Chen, X.L. Jiao, J. Phys. Chem. B 110 (2006) 2668.
[14] J. Tang, Z. Zou, J. Ye, Chem. Mater. 16 (2004) 1644.
[15] J. Tang, Z. Zou, J. Ye, Angew. Chem., Int. Ed. 43 (2004) 4463.
[16] S. Ouyang, H. Zhang, D. Li, T. Yu, J. Ye, Z. Zou, J. Phys. Chem. B 110 (2006) 11677.
[17] Y. Maruyama, H. Irie, K. Hashimoto, J. Phys. Chem. B 110 (2006) 23274.
[18] H. Kawazoe, M. Yasukawa, H. Hyodo, M. Kurita, H. Yanagi, M. Yasukawa, H. Hosono, Nature 389 (1997) 939.
[19] H. Yanagi, H. Kawazoe, A. Kudo, M. Yasukawa, H. Hosono, J. Electroceram. 4 (2000) 407.
[20] W. Staehlin, H.R. Oswald, Z. Anorg. Allg. Chem. 373 (1970) 69.
[21] C.T. Prewitt, R.D. Shannon, D.B. Rogers, Inorg. Chem. 10 (1971) 719.
[22] H. Yanagi, S. Inoue, K. Ueda, H. Kawazoe, H. Hosono, J. Appl. Phys. 88 (2000) 4159.
[23] J. Robertson, P.W. Peacock, M.D. Towler, R. Needs, Thin Solid Films 411 (2002) 96.
[24] M. Shimode, M. Sasaki, K. Mukaida, J. Solid State Chem. 151 (2000) 16.
[25] B.U. Koehler, M. Jansen, Z. Kristallogr. 165 (1983) 313.
[26] W.J. Croft, N.C. Tombs, R.E. England, Acta Crystallogr., Sect. A 17 (1964) 313.
[27] W.C. Sheets, E.S. Stampler, M.I. Bertoni, M. Sasaki, T.J. Marks, T.O. Mason, K.R. Poeppelmeier, Inorg. Chem. 46 (2007) 10741.
[28] W.C. Sheets, E. Mugnier, A. Barnabe, T.J. Marks, K.R. Poeppelmeier, Chem. Mater. 18 (2006) 7.
[29] D. Shahriari, N. Erdman, U. Haug, M. Zarzyczny, L. Marks, K. Poeppelmeier, J. Phys. Chem. Solids 64 (2003) 1437.
[30] R.D. Shannon, D.B. Rogers, C.T. Prewitt, Inorg. Chem. 10 (1971) 713.
[31] A. Buljan, P. Alemany, E. Ruiz, J. Phys. Chem. B 103 (1999) 8060.
[32] M.A. Butler, J. Appl. Phys. 48 (1977) 1914.
[33] P. Lei, C. Chen, J. Yang, W. Ma, J. Zhao, L. Zang, Environ. Sci. Technol. 39 (2005) 8466.
[34] J. Bi, L. Wu, J. Li, Z. Li, X. Wang, X. Fu, Acta Mater. 55 (2007) 4699.
[35] D. Muñoz-Rojas, G. Subías, J. Fraxedas, P. Gómez-Romero, N. Casañ-Pastor, J. Phys. Chem. B 109 (2005) 6193.
[36] D. Muñoz-Rojas, G. Subías, J. Oró-Solé, J. Fraxedas, B. Martínez, M. Casas-Cabanas, J. Canales-Vázquez, J. Gonzalez-Calbet, E. García-González, R. Walton, N. Casañ-Pastor, J. Solid State Chem. 179 (2006) 3883.
[37] J. Toyir, P. Ramírez de la Piscina, J. Fierro, N. Homs, Appl. Catal. B: Environ. 34 (2001) 255.
[38] F.F. Yang, L. Fang, S.F. Zhang, J.S. Sun, Q.T. Xu, S.Y. Wu, J.X. Dong, C.Y. Kong, Appl. Surf. Sci. 254 (2008) 5481.
[39] N. Sakai, R. Wang, A. Fujishima, T. Watanabe, K. Hashimoto, Langmuir 14 (1998) 5918.
[40] J.C. Yu, J. Yu, J. Zhao, Appl. Catal. B: Environ. 36 (2002) 31.
[41] J.C. Barreto, G.S. Smith, N.H.P. Strobel, P.A. McQuillin, T.A. Miller, Life Sci. 56 (1995) 89.